

The gas phase Smiles rearrangement of anions $\text{PhO}(\text{CH}_2)_n\text{O}^-$ ($n = 2-4$). A joint theoretical and experimental approach†

Tianfang Wang,^a Nico M. M. Nibbering^b and John H. Bowie^{*a}

Received 30th April 2010, Accepted 11th June 2010

First published as an Advance Article on the web 20th July 2010

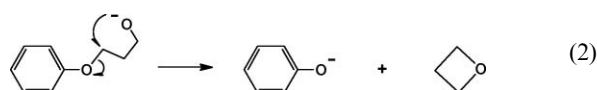
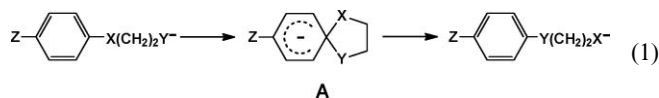
DOI: 10.1039/c0ob00064g

A combination of experimental data [using ^{18}O labelling fragmentation data together with metastable ion studies in a reverse sector mass spectrometer (from a previous study)] and *ab initio* reaction coordinate studies at the CCSD(T)/6-31++G(d,p)//B3LYP/6-31++G(d,p) level of theory, have provided the following data concerning the formation of PhO^- in the gas-phase from energized systems $\text{PhO}(\text{CH}_2)_n\text{O}^-$ ($n = 2-4$). All ΔG values were calculated at 298 K. (1) $\text{PhO}(\text{CH}_2)_2\text{O}^-$ effects an *ipso* Smiles rearrangement ($\Delta G_r = +35 \text{ kJ mol}^{-1}$; barrier to transition state $\Delta G_{\ddagger} = +40 \text{ kJ mol}^{-1}$) equilibrating the two oxygen atoms. The Smiles intermediate reverts to $\text{PhO}(\text{CH}_2)_2\text{O}^-$ which then undergoes an $\text{S}_{\text{N}}\text{i}$ reaction to form PhO^- and ethylene oxide ($\Delta G_r = -24 \text{ kJ mol}^{-1}$; $\Delta G_{\ddagger} = +54 \text{ kJ mol}^{-1}$). (2) The formation of PhO^- from energized $\text{PhO}(\text{CH}_2)_3\text{O}^-$ is more complex. Some 85% of the PhO^- formed originates *via* a Smiles intermediate ($\Delta G_r = +52 \text{ kJ mol}^{-1}$; $\Delta G_{\ddagger} = +61 \text{ kJ mol}^{-1}$). This species reconverts to $\text{PhO}(\text{CH}_2)_3\text{O}^-$ which then fragments to PhO^- by two competing processes, namely, (a) an $\text{S}_{\text{N}}\text{i}$ process yielding PhO^- and trimethylene oxide ($\Delta G_r = -27 \text{ kJ mol}^{-1}$; $\Delta G_{\ddagger} = +69 \text{ kJ mol}^{-1}$), and (b) a dissociation process giving PhO^- , ethylene and formaldehyde ($\Delta G_r = -65 \text{ kJ mol}^{-1}$; $\Delta G_{\ddagger} = +69 \text{ kJ mol}^{-1}$). The other fifteen percent of PhO^- is formed prior to formation of the Smiles intermediate, occurring directly by the $\text{S}_{\text{N}}\text{i}$ and dissociation processes outlined above. The operation of two fragmentation pathways is supported by the presence of a composite metastable ion peak. (3) Energized $\text{PhO}(\text{CH}_2)_4\text{O}^-$ fragments exclusively by an $\text{S}_{\text{N}}\text{i}$ process to form PhO^- and tetrahydrofuran ($\Delta G_r = -101 \text{ kJ mol}^{-1}$; $\Delta G_{\ddagger} = +53 \text{ kJ mol}^{-1}$). The Smiles *ipso* cyclization ($\Delta G_r = +64 \text{ kJ mol}^{-1}$; $\Delta G_{\ddagger} = +74 \text{ kJ mol}^{-1}$) is not detected in this system.

Introduction

A classical (condensed phase) Smiles rearrangement^{1,2} is shown in eqn (1). In general, this nucleophilic *ipso* attack normally requires an electron withdrawing group (*e.g.* nitro, sulfonyl or halogen) either in the *ortho* or *para* position on the aromatic ring; generally X is a good leaving group, Y is a strong nucleophile and Z is shown as a *para* substituent in eqn 1. A specific example of the condensed phase Smiles rearrangement has been reported for $\text{ArO}(\text{CH}_2)_n\text{O}^-$ [$n = 2-4$; Ar = 2,4-dinitronaphthalene], where the extent of the Smiles rearrangement decreases as n increases.² The anionic Smiles rearrangement has been used extensively synthetically (see *e.g.*³⁻⁹ for some recent examples), and radical Smiles rearrangements have also been reported.¹⁰⁻¹⁴ The Truce-Smiles rearrangement

(involving attack of a carbanion centre at an *ipso* electrophilic centre) has also been used as a synthetic method.^{15,16}

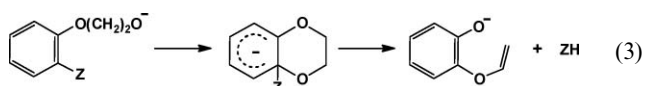


The gas phase Smiles rearrangement has not been studied as comprehensively as that in the condensed phase. The gas-phase Smiles rearrangement occurs without the necessity for activation of the aromatic ring by electron-withdrawing groups. Heavy atom (^{13}C and ^{18}O) labelling and metastable ion studies (i) show that the product ion PhO^- from $\text{PhO}(\text{CH}_2)_2\text{O}^-$ and products PhO^- and PhS^- from $\text{PhS}(\text{CH}_2)_2\text{O}^-$ are formed exclusively *via* Smiles intermediates A ($\text{X}=\text{Y}=\text{O}$ or $\text{X}=\text{S}$, $\text{Y}=\text{O}$), (ii) suggest that the formation of PhO^- from $\text{PhO}(\text{CH}_2)_3\text{O}^-$ occurs *via* competitive Smiles (85%) and $\text{S}_{\text{N}}\text{i}$ reactions (eqn (2), 15%), and (iii), indicate that PhO^- is formed from $\text{PhO}(\text{CH}_2)_4\text{O}^-$ solely by an $\text{S}_{\text{N}}\text{i}$ process.¹⁷ ^{18}O Labelling shows that when there is a substituent in the *ortho* position, the gas phase Smiles rearrangement competes with an *ortho* cyclization process,¹⁸ perhaps as shown in eqn (3). The classical $[\text{PhNO}_2]^-$ to $[\text{PhONO}]^-$ gas phase rearrangement is probably an *ipso* process,¹⁹ and gas-phase Smiles processes have been proposed for 2-hydroxybenzyl-*N*-pyrimidinylamine,²⁰ phenoxy-*N*-phenyl acetamide anions,²¹ deprotonated 2-(4,6-dimethoxypyrimidine-2-ylsulfanyl)-*N*-phenylbenzamide²² and other systems.²³⁻²⁶

^aDepartment of Chemistry, The University of Adelaide, South Australia 5005. E-mail: john.bowie@adelaide.edu.au

^bLaser Centre and Chemistry Department, Vrije Universiteit, De Boelelaan 1083, 1081 HV Amsterdam, The Netherlands. E-mail: nibberin@chem.vu.nl

† Electronic supplementary information (ESI) available: Table S1 - Geometries and energies of all species shown in Fig. 1. Smiles and $\text{S}_{\text{N}}\text{i}$ reactions of $\text{PhO}(\text{CH}_2)_2\text{O}^-$. CCSD(T)/6-31++G(d,p)//B3LYP/6-31++G(d,p) level of theory. Table S2 - Geometries and energies of all species shown in Fig. 2. Smiles and $\text{S}_{\text{N}}\text{i}$ reactions of $\text{PhO}(\text{CH}_2)_3\text{O}^-$. CCSD(T)/6-31++G(d,p)//B3LYP/6-31++G(d,p) level of theory. Table S3 - Geometries and energies of all species shown in Fig. 3. Smiles and $\text{S}_{\text{N}}\text{i}$ reactions of $\text{PhO}(\text{CH}_2)_4\text{O}^-$. CCSD(T)/6-31++G(d,p)//B3LYP/6-31++G(d,p) level of theory. Table S4 - Geometries and energies of all species shown in Fig. 5. CCSD(T)/6-31++G(d,p)//B3LYP/6-31++G(d,p) level of theory. Table S5 - Geometries and energies of all species shown in Fig. 6. CCSD(T)/6-31++G(d,p)//B3LYP/6-31++G(d,p) level of theory. See DOI: 10.1039/c0ob00064g



When we first reported the gas phase Smiles rearrangement, as in eqn (1), the conclusions of the experimental study were based primarily on heavy atom labelling data. We did not then have access to supercomputers capable of handling high-level calculations of molecules containing phenyl rings. We now report the behaviour of the energized anion systems $\text{PhO}(\text{CH}_2)_n\text{O}^-$ ($n = 2, 3$ and 4) using *ab initio* calculations at the CCSD(T)/6-31++G(d,p)//B3LYP/6-31++G(d,p) level of theory. The results of these calculations are used to complement the earlier experimental results in order to explore the mechanisms for the formation of PhO^- from these three related systems.

Results and Discussion

The results of the CCSD(T)/6-31++G(d,p)//B3LYP/6-31++G(d,p) calculations for the formation of PhO^- from $\text{PhO}(\text{CH}_2)_n\text{O}^-$ ($n = 2$ and 4) systems are in accord with the experimental results reported earlier for these two systems. All ΔG values recorded in the text and Figs were calculated at 298 K.

The theoretical results for those processes of $\text{PhOCH}_2\text{CH}_2\text{O}^-$ which result in the formation of the phenoxide anion (PhO^-) are summarised in Fig. 1, with full details of geometries and energies of minima and transition states for the species (shown in Fig. 1) recorded in Table S1.† Kinetically favoured process A involves the formation of Smiles intermediate 2 ($\Delta G_r = +35 \text{ kJ mol}^{-1}$) from $\text{PhOCH}_2\text{CH}_2\text{O}^-$ (1). The reaction proceeds *via* stable conformer

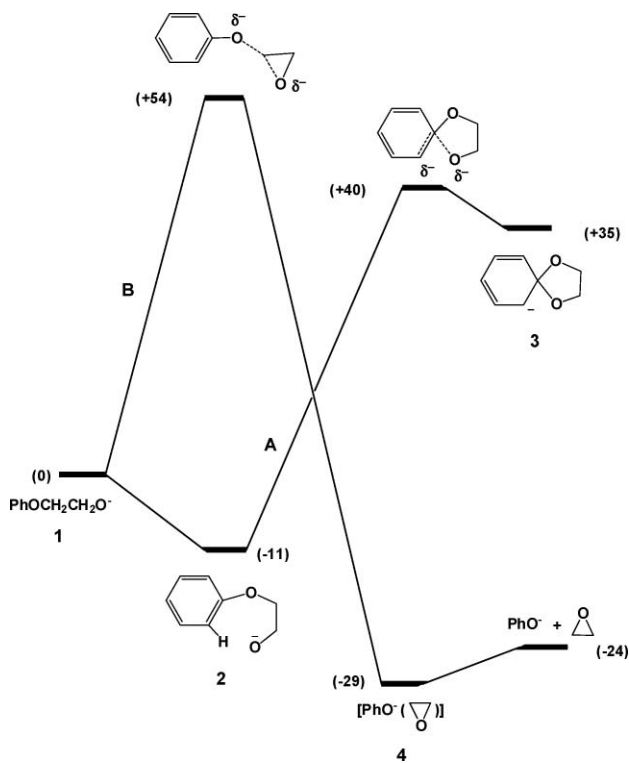


Fig. 1 Smiles and S_{Ni} reactions of $\text{PhO}(\text{CH}_2)_2\text{O}^-$. CCSD(T)/6-31++G(d,p)//B3LYP/6-31++G(d,p) level of theory. Relative energies (ΔG at 298 K). Further details of energies and geometries are contained in Table S1.†

2 over Smiles transition state 2/3 (+40 kJ mol^{-1}). S_{Ni} Process B occurs from 1 over a transition state 1,4 (barrier 54 kJ mol^{-1}) to form ion-neutral complex 4 (-29 kJ mol^{-1}) which dissociates to PhO^- and ethylene oxide in a reaction favourable by -24 kJ mol^{-1} . There is no low-energy process by which Smiles intermediate 3 synchronously forms PhO^- and ethylene oxide. Thus Smiles intermediate 3 is formed first by route A, followed by ring opening of 3 to give $\text{PhOCH}_2\text{CH}_2\text{O}^-$ (in which the two oxygens are now “equilibrated”) which then may fragment (by route B) to yield PhO^- and ethylene oxide.

The situation concerning the formation of PhO^- from $\text{PhO}(\text{CH}_2)_4\text{O}^-$ is summarized in Fig. 2 with energies and geometries of all species (shown in Fig. 2) listed in Table S2.† In this system, S_{Ni} process D is both kinetically and thermodynamically favoured. Smiles process C proceeds through intermediate 6 (+14 kJ mol^{-1}) over transition state 6/7 (+74 kJ mol^{-1}) to Smiles intermediate 7 in a reaction unfavourable by +64 kJ mol^{-1} . Favoured S_{Ni} process D occurs from $\text{PhO}(\text{CH}_2)_4\text{O}^-$ (5) over transition state 5/8 (+53 kJ mol^{-1}), to ion-neutral complex 8 (-113 kJ mol^{-1}) which dissociates to PhO^- and tetrahydrofuran. The overall process is favourable by 101 kJ mol^{-1} . These data are in accord with previous experimental data which indicate that energized $\text{Ph}^{16}\text{O}(\text{CH}_2)_4^{18}\text{O}^-$ fragments to yield only Ph^{16}O^- .¹⁷ Thus theory and experiment confirm that the Smiles rearrangement is not involved in this system.

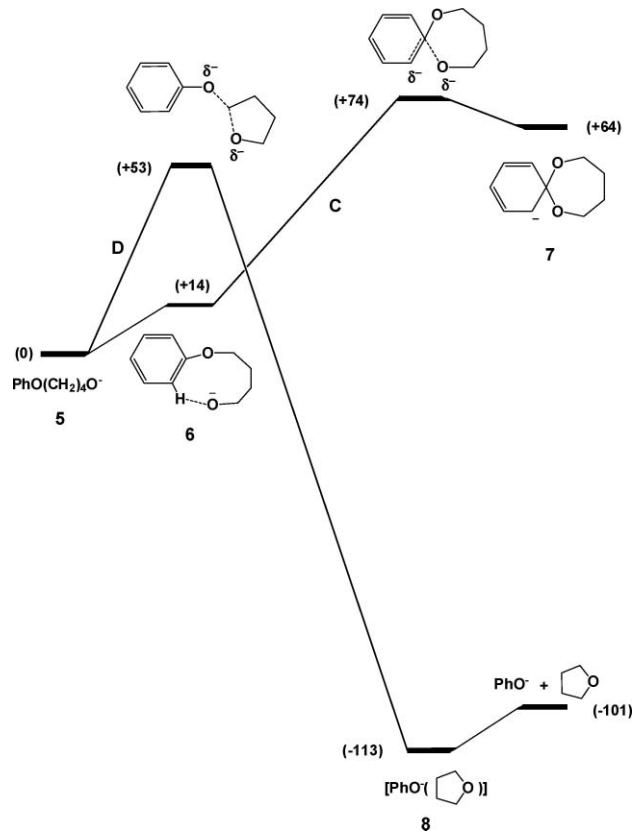


Fig. 2 Smiles and S_{Ni} reactions of $\text{PhO}(\text{CH}_2)_4\text{O}^-$. CCSD(T)/6-31++G(d,p)//B3LYP/6-31++G(d,p) level of theory. Relative energies (ΔG at 298 K). Further details of energies and geometries are contained in Table S2.†

The Smiles and $S_{\text{N}}\text{i}$ processes of $\text{PhO}(\text{CH}_2)_3\text{O}^-$ are shown in Fig. 3 with full energy and geometry data for all species (shown in Fig. 3) listed in Table S3.† From experimental results reported previously, it has been proposed that $\text{Ph}^{16}\text{OCH}_2\text{CH}_2\text{CH}_2^{18}\text{O}^-$ fragments by two processes.¹⁷ The first, the major process, (85%), equilibrates the two oxygens yielding Ph^{16}O^- and Ph^{18}O^- in equal abundance. The minor process, (15%), yields only Ph^{16}O^- , which does not involve equilibration of the two oxygens. In principle, the data shown in Fig. 3 fit this scenario. Process E, the Smiles process, ($9 \rightarrow 10 \rightarrow 11 \rightarrow 12 \rightarrow \text{PhO}^-$) is kinetically favoured with the barrier to transition state $10/11$ of +61 kJ mol^{-1} . This suggests the Smiles cyclization is the major process which equilibrates the oxygens. The $S_{\text{N}}\text{i}$ process F ($9 \rightarrow 12 \rightarrow \text{PhO}^-$) has a barrier to transition state $9/12$ of 69 kJ mol^{-1} , a value close enough to the barrier of process E (+61 kJ mol^{-1}) to accommodate the possibility of minor formation of PhO^- by process F.

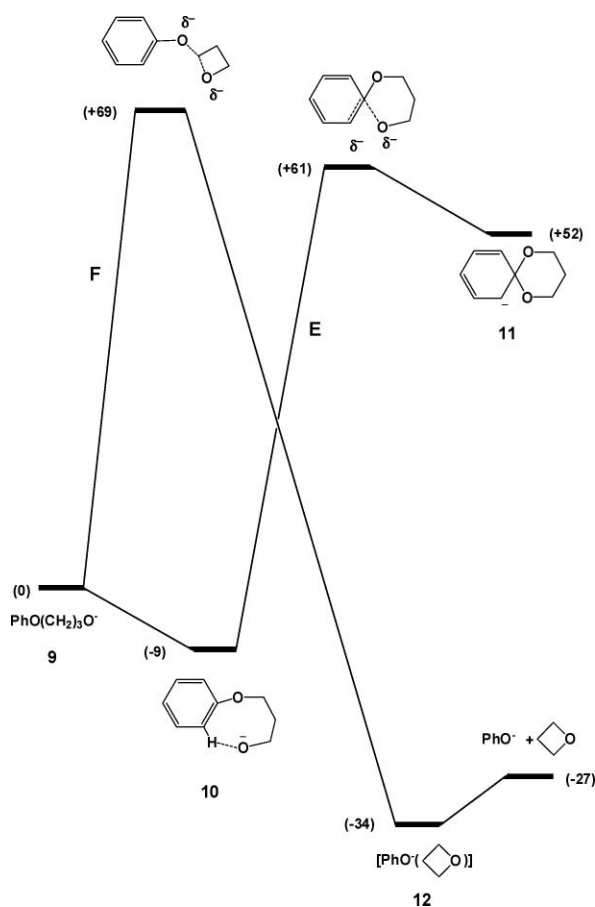


Fig. 3 Smiles and $S_{\text{N}}\text{i}$ reactions of $\text{PhO}(\text{CH}_2)_3\text{O}^-$. CCSD(T)/6-31++G(d,p)//B3LYP/6-31++G(d,p) level of theory. Relative energies (ΔG at 298 K). Further details of energies and geometries are contained in Table S3.†

But there may be a potential problem. We reported previously that when PhO^- is formed by a single process, that process is characterized by a broad Gaussian shaped metastable ion peak.¹⁷ This is the case for both the Smiles/ $S_{\text{N}}\text{i}$ sequence of $\text{PhO}(\text{CH}_2)_2\text{O}^-$ (cf. Fig. 1) and the $S_{\text{N}}\text{i}$ process of $\text{PhO}(\text{CH}_2)_4\text{O}^-$ (cf. Fig. 2). In contrast, the formation of PhO^- from energized $\text{PhO}(\text{CH}_2)_3\text{O}^-$ shows a composite metastable ion; a major Gaussian peak superimposed on a broader peak. Comparison of the metastable

ion profiles for PhO^- formed from $\text{PhO}(\text{CH}_2)_n\text{O}^-$ ($n = 2$ and 3) are shown in Fig. 4. A similar broad and composite metastable peak is also observed for the formation of PhS^- from $\text{PhS}(\text{CH}_2)_3\text{O}^-$, whereas single (and broad) Gaussian peaks are observed for the formation of PhS^- from the cognate species $\text{PhS}(\text{CH}_2)_n\text{O}^-$ ($n = 2$ and 4) (data not provided here, but see¹⁷). A composite metastable ion indicates the operation of several different routes to PhO^- from $\text{PhO}(\text{CH}_2)_3\text{O}^-$. Is this merely a consequence of the direct and indirect formation of PhO^- by the $S_{\text{N}}\text{i}$ process as shown in Fig. 4, with accompanying different values of kinetic energy release? Alternatively, is there something unique about the $\text{PhO}(\text{CH}_2)_3\text{O}^-$ system which suggests a pathway to PhO^- different from the Smiles and/or $S_{\text{N}}\text{i}$ processes shown in Fig. 3?

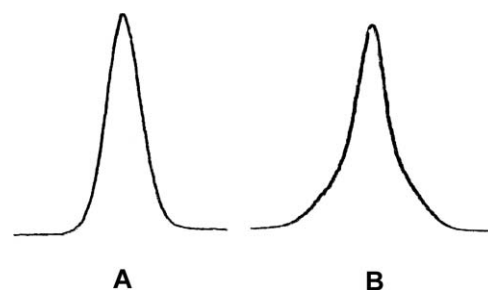


Fig. 4 Metastable anion profiles for the formation of PhO^- from (a) $\text{PhO}(\text{CH}_2)_2\text{O}^-$ (width of peak at half height = $40.5 \pm 0.5\text{V}$) and (b) $\text{PhO}(\text{CH}_2)_3\text{O}^-$ (major component half width, ca. 35V), from ref.¹⁷ VG ZAB 2HF mass spectrometer. For full experimental details see Ref. 17

In agreement with the situation outlined above for $\text{PhO}(\text{CH}_2)_2\text{O}^-$, there is no low-energy and synchronous formation of PhO^- from Smiles intermediate **11** (Fig. 3), so formation of PhO^- directly from **11** is not a possible option. However, a feature of this system not available for those shown in Fig. 1 and 2 is that $\text{PhO}(\text{CH}_2)_3\text{O}^-$ can, in principle, form a hydride complex $[(\text{PhOCH}_2\text{CH}_2\text{CHO})\text{H}]^-$, in which the hydride ion can initiate an elimination reaction to produce PhO^- , $\text{CH}_2=\text{CHCHO}$ and H_2 , and/or an $S_{\text{N}}2$ process within the anion complex to form PhO^- and $\text{CH}_3\text{CH}_2\text{CHO}$. The latter process can, in principle, also occur for $\text{PhO}(\text{CH}_2)_n\text{O}^-$ ($n = 2$ and 4). A final process for consideration is the possible decomposition of $\text{PhO}(\text{CH}_2)_3\text{O}^-$ to yield PhO^- , $\text{CH}_2=\text{CH}_2$ and CH_2O . The reaction coordinate profiles of these three reactions have been investigated and are summarized in Fig. 5 and 6, with details of energies and geometries of all species shown in Fig. 5 and 6 recorded in Tables S4 and S5.†

The $S_{\text{N}}2$ H^- and elimination mechanisms are depicted as processes **G** and **H** in Fig. 5. Both processes are favourable with ΔG_{r} being negative. However, both are kinetically unfavourable (with respect to the two processes shown in Fig. 4) with barriers to transition states $9/13$ and $9/14$ of +151 and +139 kJ mol^{-1} , respectively. There is no hydride ion-neutral complex present on either reaction coordinate. The $S_{\text{N}}2$ reaction is synchronous to anion-neutral complex **13**, which dissociates to yield PhO^- and $\text{CH}_3\text{CH}_2\text{CHO}$ in a reaction sequence favourable by 140 kJ mol^{-1} . The elimination reaction is synchronous to anion-neutral complex **14**, which decomposes to produce PhO^- together with acetaldehyde and dihydrogen in a reaction favourable by 56 kJ mol^{-1} .

The final process for consideration is depicted as route **I** in Fig. 6. This process is also favourable ($\Delta G_{\text{r}} = -65 \text{ kJ mol}^{-1}$), but in this case the barrier to transition state $9/15$ is only

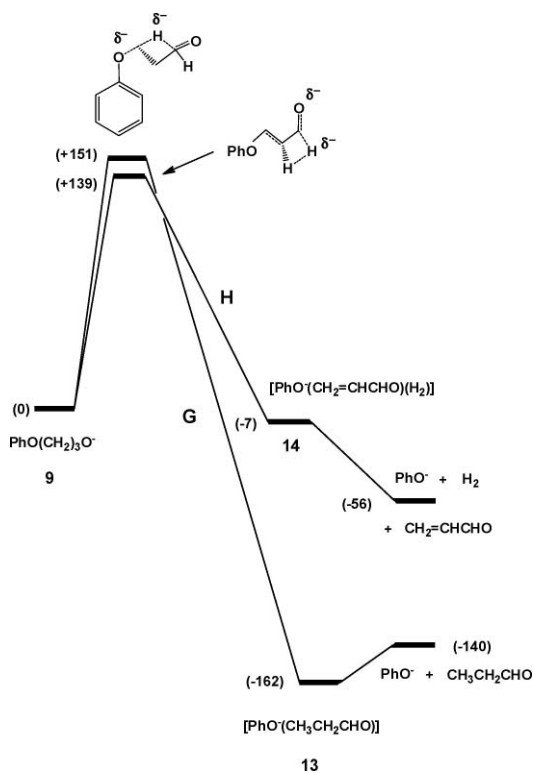


Fig. 5 S_N2 and elimination potential profiles for the formation of PhO^- from $\text{PhO}(\text{CH}_2)_3\text{O}^-$. CCSD(T)/6-31++G(d,p)//B3LYP/6-31++G(d,p) level of theory. Relative energies (ΔG at 298 K). Further details of energies and geometries are contained in Table S4.†

74 kJ mol^{-1} : a value of the same order as those shown in Fig. 3 for the Smiles process (+61 kJ mol^{-1}) and the S_{Ni} process +69 kJ mol^{-1}). The proposed pathways for the formation of PhO^- from $\text{PhO}(\text{CH}_2)_3\text{O}^-$ are summarised in Scheme 1. Eighty five percent of the product PhO^- is formed following oxygen equilibration through the Smiles intermediate. Reversal of the Smiles reaction reforms $\text{PhO}(\text{CH}_2)_3\text{O}^-$ which can then fragment to give PhO^- by the S_{Ni} and dissociation processes. Fifteen percent of PhO^- formation proceeds without equilibration of the oxygens and may occur directly from $\text{PhO}(\text{CH}_2)_3\text{O}^-$ by a combination of the S_{Ni} and dissociation processes. The operation of the S_{Ni} and dissociation processes shown in Scheme 1 are consistent with the composite metastable ion shown in Fig. 4. It is not known which of these two processes produces the narrower component of the composite metastable ion peak.‡

‡ Predicting the relative kinetic energy releases which accompany particular negative ion decompositions in the gas phase (from the relative peak widths of their metastable ions at half height) is sometimes not straightforward. Skeletal rearrangements, retro cleavages, loss of an olefin with H transfer, and internal cyclization reactions of negative ions can give either broad or dish-shaped metastable peaks with half heights ranging anywhere from 70–170 V.^{27–30} Similar processes from different anions can give quite different metastable peak profiles: for example, the losses of water from the (M-H)⁻ ions of 1-hydroxycyclohex-2-ene³¹ and 2-(oxiran-2-yl)ethan-1-ol³² show a narrow Gaussian peak (half height = 29V) and a dish-shaped peak (half height = 72V) respectively. Simple cleavage processes normally exhibit narrow metastable peaks (< 35V),^{27–32} but there are exceptions with broad Gaussian metastable peaks sometimes being encountered for simple cleavages.³³

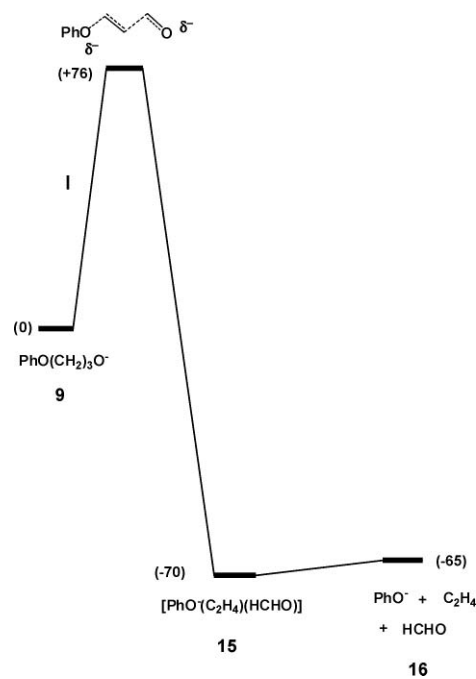
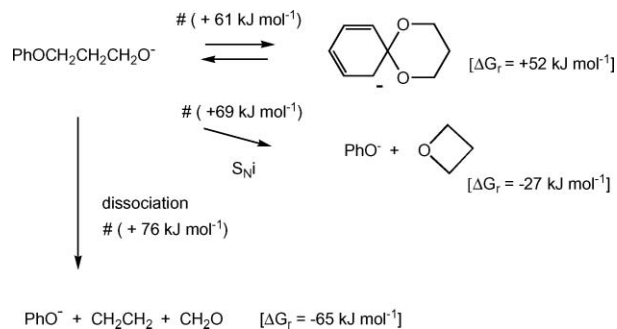


Fig. 6 Dissociation potential profile for the formation of PhO^- , CH_2CH_2 and CH_2O from $\text{PhO}(\text{CH}_2)_3\text{O}^-$. CCSD(T)/6-31++G(d,p)//B3LYP/6-31++G(d,p) level of theory. Relative energies (ΔG at 298 K). Further details of energies and geometries are contained in Table S5.†



Scheme 1

Conclusions

A combination of (previous) experimental evidence and (current) theoretical data provide the following information:-

(1) Energized $\text{PhO}(\text{CH}_2)_2\text{O}^-$ undergoes *ipso* rearrangement in the gas phase to form a Smiles intermediate which reconverts to $\text{PhO}(\text{CH}_2)_2\text{O}^-$ which then effects an S_{Ni} cyclization to yield PhO^- and ethylene oxide.

(2) Energized $\text{PhO}(\text{CH}_2)_3\text{O}^-$ undergoes a number of competitive reactions. The major process (85%) involves a Smiles rearrangement. The Smiles intermediate may revert to $\text{Ph}(\text{CH}_2)_3\text{O}^-$ which can then fragment to yield the anion PhO^- by two competitive processes; namely (i) an S_{Ni} process to form PhO^- and trimethylene oxide, and (ii) a dissociation process to give PhO^- , ethylene and formaldehyde. Fifteen percent of the anions PhO^- are formed by direct decomposition of $\text{Ph}(\text{CH}_2)_3\text{O}^-$ (without intervention of a Smiles intermediate) by a combination of the S_{Ni} and dissociation routes outlined above.

(3) Energized $\text{PhO}(\text{CH}_2)_4\text{O}^-$ does not undergo Smiles rearrangement. Instead, it fragments following exclusive $\text{S}_{\text{N}}1$ cyclization to yield PhO^- and tetrahydrofuran.

Theoretical methods

Geometry optimizations were carried out by using the B3LYP^{34,35} functional with the 6-31++G(d,p) basis set. Stationary points were characterized as either minima (no imaginary frequencies) or transition states (one imaginary frequency) by calculation of the frequencies using analytical gradient procedures. The minima connected by a given transition structure were confirmed by intrinsic reaction coordinate (IRC) calculations.³⁶ The nature of the stationary points and the zero point energy corrections were examined by calculating the Hessian matrix at the B3LYP/6-31++G(d,p) level. Single-point energies for the B3LYP/6-31++G(d,p) geometries were determined using a coupled-cluster single, double, and (perturbative) triple excitation frozen-core method, CCSD(T),³⁷ in conjunction with a 6-31++G(d,p) basis set, including zero-point energy correction (unscaled). These calculations were performed using the GAUSSIAN suite of programs.³⁸ ΔG values recorded in the text and Figs were calculated at 298 K.

Acknowledgements

We thank the Australian Research Council for financing our negative ion mass spectrometry programme. TW thanks the ARC for a research associate stipend. We thank the Australian Partners for Advanced Computing (Australian National University) and eResearch SA (The University of Adelaide) for generous allocations of supercomputer time.

References

- 1 L. A. Warren and S. Smiles, *J. Chem. Soc.*, 1930, 956; L. A. Warren and S. Smiles, *J. Chem. Soc.*, 1930, 1327; C. S. McClement and S. Smiles, *J. Chem. Soc.*, 1937, 1016; W. E. Truce, E. M. Kreider and W. W. Brand, *Org. React.*, 1970, **18**, 99; C. F. Bernasconi and H.-C. Wang, *J. Am. Chem. Soc.*, 1976, **98**, 6265; D. M. Schmidt and G. E. Bonvicino, *J. Org. Chem.*, 1984, **49**, 1664 and references cited therein.
- 2 M. R. Crampton and M. J. Willison, *J. Chem. Soc., Perkin Trans. 2*, 1976, 155.
- 3 D. G. Musaev, A. L. Galloway and F. M. Menger, *THEOCHEM*, 2004, **679**, 45; L. H. Mitchell and N. C. Barvian, *Tetrahedron Lett.*, 2004, **45**, 5669.
- 4 M. Mizuno and M. Yamano, *Org. Lett.*, 2005, **7**, 3629.
- 5 L. El Kain, M. Gizolme and L. Grimaud, *Org. Lett.*, 2006, **8**, 5021.
- 6 J. B. Xiang, L. Y. Zheng and H. X. Lie, *Tetrahedron*, 2008, **64**, 9101.
- 7 H. Zho, L. J. Meng and M. Ghatai, *Tetrahedron Lett.*, 2008, **49**, 3827.
- 8 J. B. Xiang, H. X. Xie and D. S. Wen, *J. Org. Chem.*, 2008, **73**, 3281.
- 9 J. H. Li and J. S. Wang, *Aust. J. Chem.*, 2009, **62**, 176.
- 10 W. B. Motherwell and A. M. K. Pannell, *J. Chem. Soc., Chem. Commun.*, 1991, 877.
- 11 R. Caddick, C. L. Shering and S. N. Wadman, *Tetrahedron*, 2000, **56**, 465.
- 12 Ryokawa and H. Togo, *Tetrahedron*, 2001, **57**, 5915.
- 13 M. Tada, H. Shijuna and M. Nakamura, *Org. Biomol. Chem.*, 2003, **1**, 2499.
- 14 E. Bacque, M. El Qacenci and S. Z. Zard, *Org. Lett.*, 2005, **7**, 3817.
- 15 T. J. Snape, *Chem. Soc. Rev.*, 2008, **37**, 2452.
- 16 T. J. Snape, *Syn. Lett.*, 2008, 2689.
- 17 P. C. H. Eichinger, J. H. Bowie and R. N. Hayes, *J. Am. Chem. Soc.*, 1989, **111**, 4224.
- 18 P. C. H. Eichinger and J. H. Bowie, *Org. Mass Spectrom.*, 1992, **27**, 995.
- 19 J. H. Bowie, *Aust. J. Chem.*, 1971, **24**, 989.
- 20 H. Y. Wang, X. Zhang, Y.-L. Guo and L. Lu, *J. Am. Soc. Mass Spectrom.*, 2005, **16**, 1561.
- 21 F. Wang, *Rapid Commun. Mass Spectrom.*, 2006, **20**, 1820.
- 22 Y. P. Zhou, Y. J. Pan and X. T. Cao, *J. Chem. Soc., Perkin Trans. 2*, 1998, 1629.
- 23 M. Shafi, M. Hussain and S. G. Peeran, *Phosphorus, Sulfur Silicon Relat. Elem.*, 2007, **182**, 2087.
- 24 M. J. Sun, W. Daim and D. Q. Liu, *J. Mass Spectrom.*, 2008, **43**, 383.
- 25 P. H. Lambert, S. Berlin, J. M. Lacoste, J. P. Volland, A. Krick, E. Furet, A. Botrel and P. Guenot, *J. Mass Spectrom.*, 1998, **33**, 242.
- 26 M. J. Maclean, S. Walker, T. Wang, P. C. H. Eichinger, P. J. Sherman and J. H. Bowie, *Org. Biomol. Chem.*, 2010, **8**, 371.
- 27 P. C. H. Eichinger and J. H. Bowie, *J. Chem. Soc., Perkin Trans. 2*, 1990, 1763.
- 28 R. J. Waugh, R. N. Hayes, P. C. H. Eichinger, K. M. Downard and J. H. Bowie, *J. Am. Chem. Soc.*, 1990, **112**, 2537.
- 29 P. C. H. Eichinger, R. N. Hayes and J. H. Bowie, *J. Chem. Soc. Perkin Trans.*, 1990, **2**, 1815.
- 30 G. W. Adams, J. H. Bowie and R. N. Hayes, *Int. J. Mass Spectrom. Ion Processes*, 1992, **114**, 163.
- 31 S. Dua, R. B. Whait, M. J. Alexander, R. N. Hayes, A. T. Lebedev, P. C. H. Eichinger and J. H. Bowie, *J. Am. Chem. Soc.*, 1993, **115**, 5709.
- 32 J. M. Hevko, S. Dua, M. S. Taylor and J. H. Bowie, *J. Chem. Soc. Perkin Trans.*, 1998, **2**, 1629.
- 33 M. J. Raftery and J. H. Bowie, *Int. J. Mass Spectrom. Ion Processes*, 1988, **85**, 167.
- 34 A. D. Becke, *Phys. Rev. A: At., Mol., Opt. Phys.*, 1988, **38**, 3098.
- 35 C. T. Lee, W. T. Yang and R. G. Parr, *Phys. Rev. B: Condens. Matter*, 1988, **37**, 785.
- 36 K. Fukui, *Acc. Chem. Res.*, 1981, **14**, 363.
- 37 (a) T. H. Dunning, *J. Chem. Phys.*, 1989, **90**, 1007; (b) D. E. Woon and T. H. Dunning, *J. Chem. Phys.*, 1993, **98**, 1358.
- 38 M. J. Frisch, G. W. Trucks, H. B. Schlegel, G. E. Scuseria, M. A. Robb, J. R. Cheeseman, J. A. Montgomery, T. Vreven, K. N. Kudin, J. C. Burant, J. M. Millam, S. S. Iyengar, J. Tomasi, V. Barone, B. Mennucci, M. Cossi, G. Scalmani, N. Rega, G. A. Petersson, H. Nakatsuji, M. Hada, M. Ehara, K. Topyota, R. Fukuda, J. Hasegawa, M. Ishida, T. Makajima, Y. Honda, O. Kitao, H. Nakai, M. Klene, X. Li, J. E. Know, H. P. Hratchian, J. B. Cross, V. Bakken, C. Adamo, J. Jaramillo, R. Gomperts, R. E. Stratmann, O. Yazyev, A. J. Austin, R. Cammi, C. Pomelli, J. W. Ochterski, P. Y. Ayala, K. Morokuma, G. A. Voth, P. Salvador, J. J. Dannenberg, V. G. Zakrzewski, S. Dapprich, A. D. Daniels, M. C. Strain, O. Farkas, D. K. Malick, A. D. Rabuck, K. Raghavachari, J. B. Foresman, J. V. Ortiz, Q. Cui, A. G. Baboul, S. Clifflors, J. Cioslowski, B. B. Stefanov, G. Liu, A. Liashenko, P. Piskorz, I. Komaromi, R. L. Martin, D. J. Fox, T. Keith, M. A. Al-Latham, C. Y. Peng, A. Nanayakkara, M. Challacombe, P. M. W. Gill, B. Johnson, W. Chen, M. W. Wong, C. Gonzalez, J. A. Pople, *Gaussian 03, Revision E*, Gaussian, Inc.: Wallingford, CT, 2004.